Environmental Pollution 342 (2024) 123047

Contents lists available at ScienceDirect

Environmental Pollution

journal homepage: www.elsevier.com/locate/envpol

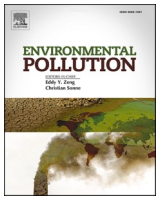

Hepatotoxicity of cyanotoxin microcystin-LR in human: Insights into mechanisms of action in the 3D culture model Hepoid-HepaRG☆

Riju R. Chowdhury [a], Sophie Rose [b], Frédéric Ezan [b], Iva Sovadinová [a], Pavel Babica [a,1], Sophie Langouët [b,*,1]

[a] Masaryk University, Faculty of Science, RECETOX, Kotlářská 2, 61137, Brno, Czech Republic
[b] University of Rennes, Inserm, EHESP, Irset (Institut de Recherche en santé, environnement et travail), UMR_S 1085, 35000, Rennes, France

ARTICLE INFO

Keywords:
Cyanotoxins
Microcystin-LR
3D human liver model Hepoid-HepaRG
Organic anion transporting polypeptides
Hepatocarcinogenesis

ABSTRACT

Microcystin-LR (MC-LR) is a potent hepatotoxin produced by harmful cyanobacterial blooms (CyanoHABs). MC-LR targets highly differentiated hepatocytes expressing organic anion transporting polypeptides OATP1B1 and OATP1B3 that are responsible for hepatocellular uptake of the toxin. The present study utilized an advanced 3D *in vitro* human liver model Hepoid-HepaRG based on the cultivation of collagen-matrix embedded multicellular spheroids composed of highly differentiated and polarized hepatocyte-like cells. 14-d-old Hepoid-HepaRG cultures showed increased expression of OATP1B1/1B3 and sensitivity to MC-LR cytotoxicity at concentrations >10 nM (48 h exposure, EC_{20} = 26 nM). MC-LR induced neither caspase 3/7 activity nor expression of the endoplasmic reticulum stress marker gene BiP/GRP78, but increased release of pro-inflammatory cytokine IL-8, indicating a necrotic type of cell death. Subcytotoxic (10 nM) and cytotoxic (≥100 nM) MC-LR concentrations disrupted hepatocyte functions, such as xenobiotic metabolism phase-I enzyme activities (cytochrome P450 1A/1B) and albumin secretion, along with reduced expression of *CYP1A2* and *ALB* genes. MC-LR also decreased expression of *HNF4A* gene, a critical regulator of hepatocyte differentiation and function. Genes encoding hepatobiliary membrane transporters (OATP1B1, BSEP, NTCP), hepatocyte gap junctional gene connexin 32 and the epithelial cell marker E-cadherin were also downregulated. Simultaneous upregulation of connexin 43 gene, primarily expressed by liver progenitor and non-parenchymal cells, indicated a disruption of tissue homeostasis. This was associated with a shift in the expression ratio of E-cadherin to N-cadherin towards the mesenchymal cell marker, a process linked to epithelial-mesenchymal transition (EMT) and hepatocarcinogenesis. The effects observed in the human liver cell *in vitro* model revealed mechanisms that can potentially contribute to the MC-LR-induced promotion and progression of hepatocellular carcinoma (HCC). Hepoid-HepaRG cultures provide a robust, accessible and versatile *in vitro* model, capable of sensitively detecting hepatotoxic effects at toxicologically relevant concentrations, allowing for assessing hepatotoxicity mechanisms, human health hazards and impacts of environmental hepatotoxins, such as MC-LR.

1. Introduction

Harmful cyanobacterial blooms (CyanoHABs), intensified by nutrient over-enrichment or climate change, represent a growing threat to ecosystems and public health. Consequently, cyanobacterial toxins (cyanotoxins) increasingly contaminate various environmental compartments, including aquatic ecosystems, drinking water sources, sediments, soils, and atmospheric aerosols (Lad et al., 2022; Plaas and Paerl, 2021). Microcystins are probably the most prevalent cyanotoxins in the environment, with microcystin-LR (MC-LR) representing one of the most common and toxic congeners (Lad et al., 2022; Plaas and Paerl, 2021). Microcystins primarily target highly differentiated polarized hepatocytes expressing in their sinusoidal membranes organic anion transporting polypeptides (OATPs) isoforms 1B1 and 1B3, that are responsible for the cellular uptake of microcystins (Fischer et al., 2005). Microcystins inhibit protein phosphatases 1 and 2A, resulting in the

☆ This paper has been recommended for acceptance by Wen Chen.

* Corresponding author.
E-mail address: sophie.langouet@inserm.fr (S. Langouët).

[1] These authors contributed equally to this work.

https://doi.org/10.1016/j.envpol.2023.123047
Received 10 August 2023; Received in revised form 3 November 2023; Accepted 23 November 2023
Available online 29 November 2023

hyperphosphorylation of intracellular proteins, which includes disruption of the cytoskeleton causing cell damage and eventually culminating in cell death by necrosis or apoptosis. Subcytotoxic doses of microcystins induce cellular stress, endoplasmic reticulum (ER) stress, oxidative stress, DNA damage, and inflammatory responses. These processes are associated with alterations in signal and gene pathways that regulate cell survival, proliferation, or migration (Lad et al., 2022; Shi et al., 2021). Microcystins function as tumor promoters, with MC-LR classified as possibly carcinogenic to humans (Group 2B) by International Agency for Research on Cancer (IARC, 2010). In the liver of exposed animals or humans, microcystins can cause acute and possibly fatal liver injury, while long-term exposures have been associated with chronic liver toxicity, including hepatic steatosis, steatohepatitis and liver cancer (Buratti et al., 2017; Lad et al., 2022; Shi et al., 2021; Svirčev et al., 2019). The World Health Organization (WHO) derived provisional short-term and lifetime guideline values for MC-LR concentrations in drinking water as 12 μg/L (~12 nM) or 1 μg/L (~1 nM), respectively (WHO, 2020).

Nevertheless, further investigations into microcystin hepatotoxicity and human health hazard assessments are largely limited when using conventional monolayer (two-dimensional, 2D) *in vitro* models of hepatic cells. In freshly isolated primary human hepatocytes (PHH) highly expressing OATPs (Kotani et al., 2012; Ulvestad et al., 2013, 2011), MC-LR typically induces significant cytotoxic effects at concentrations <100 nM (Batista et al., 2003; Fischer et al., 2010; Ufelmann et al., 2012). Compared to primary cells, 2D cultures of immortalized human hepatic cells such as HepG2 exhibit lower OATP expression (Ulvestad et al., 2013, 2011) and thus lower sensitivity to microcystin hepatocytotoxicity, often by one or several orders of magnitude (Ikehara et al., 2015; Jasionek et al., 2010; Ma et al., 2017). Three-dimensional (3D) cultures of hepatic cells have been shown to mimic the tissue-like microenvironment, cellular interactions and functions found in the liver more effectively than traditional 2D models (Bomo et al., 2016; Ingelman-Sundberg and Lauschke, 2022; Rose et al., 2021; Serras et al., 2021; Yang et al., 2021). Only a limited number of studies utilized 3D cultures to study the hepatotoxic effects of microcystins using spheroids of primary rodent hepatocytes (Battle et al., 1999; Rhee et al., 2006), human hepatoblastoma cells HepG2 (Roegner and Puschner, 2014), or human liver stem cells HL1-hT1 (Basu et al., 2018). Although these studies showed high sensitivity of 3D liver cultures to MC-LR-induced toxicity, they primarily focused on changes in morphology, cell viability or oxidative stress, but without further investigating the mechanisms underlying MC-LR-dependent toxicity, which might contribute to the development of liver diseases, including hepatocellular carcinoma (HCC).

A recently developed Hepoid-HepaRG *in vitro* model represents a robust, reproducible, and easily accessible 3D cell culture model, allowing differentiation of human HepaRG cells without any dimethylsulfoxide (DMSO) use as in conventional approaches. Instead, Hepoid-HepaRG are grown within a collagen matrix, resulting in the formation of 3D multicellular bodies composed of highly differentiated and polarized hepatocyte-like cells (Rose et al., 2022). In this study, we used the Hepoid-HepaRG model to investigate MC-LR toxicity, as a prominent CyanoHAB hepatotoxicant relying on drug membrane transporters. We demonstrated that Hepoid-HepaRG cultures were able to sensitively detect various MC-LR effects on hepatic cell viability, functions and gene expression changes that are linked to liver injury, loss of hepatocyte differentiation and function, and hepatocarcinogenesis.

2. Materials and methods

2.1. Cell culture and Hepoid-HepaRG generation

HepaRG cells were routinely maintained as published previously (Gripon et al., 2002). For all experiments, the cells were grown in William's E medium supplemented with insulin (5 μg/mL), glutamine (2 mM) (ThermoFisher Scientific, Hamburg, Germany), 10% (v/v) Fetal Bovine Serum (FBS, Capricorn Scientific, Ebsdorfergrund, Germany), penicillin (100 units/ml) and streptomycin (100 μg/ml) (Sigma-Aldrich, Munich, Germany) and hydrocortisone hemisuccinate (5×10^{-5} M) (Sigma-Aldrich). The cells were grown up to passage 18 in 100 mm Petri Dish (Corning, New York, NY) at 37 °C and 5% CO_2 humidified atmosphere. Medium was changed three times a week and the cells subcultured at 70–80% confluency.

3D Hepoid-HepaRG cultures were generated using collagen type-I from bovine skin (Sigma-Aldrich) (Rose et al, 2022 PMID: 34762139). Collagen was diluted with the culture medium to a final concentration of 1.5 mg/mL and pH adjusted to 7.4 with 0.1 N NaOH (Sigma-Aldrich). HepaRG cell suspension was added at a final concentration of 6×10^5 cells/mL and the mixture of cells and collagen was then seeded onto multi-well plates (Corning). Gels were allowed to polymerize for 1 h in the CO_2 incubator, then overlaid with a small volume of culture media and kept overnight. A volume of media equal to the collagen volume was added the next day and renewed three times a week. Chemical treatments were initiated after either 4 d for long-term treatment (7–14 d) or 14 d for short-term treatment (48 h) of Hepoid-HepaRG cultivation, by addition of exposure medium with MC-LR or control chemicals.

For comparative experiments, we also prepared 2D DMSO-differentiated HepaRG cells using a conventional protocol (Gripon et al., 2002). The cells were grown in monolayers in the proliferative phase for 14 d in regular culture medium, followed by a 14-d differentiation with the culture medium supplemented with 1.8% DMSO.

2.2. Microcystin-LR treatment

MC-LR (Enzo Life Sciences, Lausen, Switzerland) stock solution (1 mM) was prepared in sterile ultrapure water. Exposure media with 1, 10, 100, 1000 and 10000 nM MC-LR were prepared by dilution with culture medium while maintaining the solvent concentration at 1% (v/v). Sterile ultrapure water (1%, v/v) served as a solvent control for all the experiments. Exposure medium was refreshed after 24 h for 48 h treatments, or three times a week for 7 d–14 d treatments. Short-term treatments were done in FBS-free exposure medium.

2.3. Cytotoxicity assay

For dose-response curve establishment and comparative sensitivity analysis with other *in vitro* models, we employed a concentration range that extended from low concentrations (≤100 nM) effective in PHH to high (≥1000 nM) concentrations usually necessary for cytotoxicity in 2D cultures of hepatic cell lines (Ikehara et al., 2015). Cell viability was assessed using CellTiter-Glo® 3D Cell Viability Assay (Promega, Madison, WI) that measures the ATP content in the cells. The exposure medium was replaced with CellTiter-Glo® 3D Assay solution and incubated for 30 min at room temperature. The luminescence was read with 1 s/well integration time, using EnSpire multimode plate reader (PerkinElmer, Waltham, MA). Hepoid-HepaRG morphology was observed using light microscopy (Leica, Wetzlar, Germany).

2.4. Caspase-3/7 activity

Caspase-3/7 activity was measured using SensoLyte® Homogenous AMC Caspase3/7 Assay Kit (Anaspec, Fremont, CA), evaluating cleavage of a fluorogenic substrate, catalyzed by the activity of caspases 3 and 7. Hepoid-HepaRG cultures were lysed with kit's lysis buffer on ice for 10 min and caspase-3/7 substrate Ac-DEVD-AMC was added. Caspase-dependent release of AMC fluorophore was monitored kinetically for 1.5 h at 37 °C as fluorescence (354 nm/442 nm excitation/emission) by EnSpire multimode plate reader (PerkinElmer). Hepoid-HepaRG cells treated with acetaminophen (1–15 mM, 48 h) or cisplatin (33–66 μM, 24 h) were used as a negative or positive control, respectively.

2.5. Albumin and urea secretion assays

Concentrations of albumin and urea were measured in the culture medium using the Human Serum Albumin DuoSet ELISA kit (R&D Systems, Minneapolis, MN) and ChromaDazzle Urea Assay kit (Assay Genie, Dublin, Ireland), respectively. Absorbances for albumin assay were taken at 450 nm (570 nm reference) and for urea assay at 430 nm using SPECTROstar Nano microplate reader (BMG Labtech, Ortenberg, Germany).

2.6. Interleukin-8 (IL-8) secretion assays

IL-8 concentrations in the cell culture medium were measured using IL-8 Human Uncoated ELISA kit (ThermoFisher Scientific) according to the manufacturer's instructions. Absorbances for IL-8 assays were taken at 450 nm (570 nm reference) using BioTek Synergy Mx microplate reader (Agilent Technologies, Santa Clara, CA).

2.7. Measurement of cytochrome P450 (CYP) activity

Activities of CYP1A1, CYP1A2 and CYP1B1 were measured using Ethoxyresorufin O-deethylation (EROD) assay, while the activity of CYP1A2 was determined using Methoxy-resorufin O-deethylation (MROD) assay. CYP activity was evaluated with or without treatment with 5 μM 3-methylcholantrene (3-MC, Sigma-Aldrich), which was added to the cells 24-h before the assay. After phosphate-buffered saline (PBS) wash, 1.5 mM salicylamide (Sigma-Aldrich) was added to the cells to block activity of phase II conjugation enzymes. Then, the substrates 7-ethoxyresorufin or 7-methoxyresorufin (Sigma-Aldrich) were added to detect EROD or MROD activity, respectively. Substrate oxidation was measured as a fluorescence (544 nm/584 nm excitation/emission) kinetically for 20 min at 37 °C using EnSpire multimode plate reader (PerkinElmer) to determine V_{max} values (pmol/min). Cell viability was then measured by CellTiter-Glo® assay (Promega). EROD/MROD activities were normalized by relative luminescence units (RLU) from viability assay (pmol/min/RLU).

2.8. RNA extraction and real-time qPCR

Hepoid-HepaRG cells were retrieved from the gels by incubation (30 min, 37 °C) with 10 μg/mL Liberase TL (Sigma-Aldrich). RNA was extracted from PBS-washed cell pellets using NucleoSpin RNA (Macherey-Nagel, Oensingen, Switzerland) and quantified by NanoDrop ND-1000 (ThermoFisher Scientific). Reverse transcription of RNA to cDNA was done using Applied Biosystems High-Capacity cDNA reverse transcription kit (ThermoFisher Scientific). Real-time qPCR analysis was carried out with Roche Light Cycler® 480 (Roche, Basel, Switzerland) using a SensiFAST SYBR No-ROX kit (Bioline, London, UK). The sequences of all the primers used and qPCR conditions are listed in Table S1. Light Cycler 480 software and the second derivative maximum method were used to calculate the crossing point cycle (Cp) value for each gene. The target gene Cp values were normalized to the geometric mean of Cp values for two reference genes, namely, eukaryotic translation elongation factor 2 (*EEF2*) and malate dehydrogenase 1 (*MDH1*) (Vandesompele et al., 2002).

2.9. Immunohistochemistry

After 1 h fixation with 4% paraformaldehyde, the cells were embedded into paraffin blocks, cut into 4 μm sections, and stained for OATP 1B1 using mouse monoclonal antibody (sc-271157, 1:200, Santa Cruz, Heidelberg, Germany). Next, the signal was enhanced using the Ventana Rhodamine kit (Roche), followed by incubation with a secondary anti-mouse antibody (760–4310, Roche) for 16 min. Rinsed sections were mounted with Dapi Fluoromount-G (Sigma-Aldrich) and imaged using a fluorescence Eclipse Ni-E microscope (Nikon, Tokyo, Japan) with a photonic Orca R2 camera (Hamamatsu, Shizuoka, Japan).

2.10. Statistical analysis

Data from chemical treatments were normalized to the solvent control and expressed as a percentage of the control, a fraction of the control (FOC) or a fold change. Time-dependent changes in OATP expression during Hepoid-HepaRG were presented as a fold change relative to the monolayer culture of differentiated HepaRG. EROD/MROD activities were expressed as a percentage of 3-MC-induced controls. For the selected gene pairs, gene expression ratios were calculated by comparing their housekeeping gene-normalized Cp values. All the results represent a minimum of three independently repeated experiments ($n \geq 3$) with data expressed as mean ± standard deviation (SD). Values of 20% or 50% effective concentrations (EC_{20} and EC_{50}) were estimated using a four-parameter logistic regression model in GraphPad (GraphPad Software, Boston, MA). Statistical comparisons were conducted using the SigmaPlot (Systat, Palo Alto, CA). Normally distributed data (Shapiro-Wilk test) with equal variances (Equal Variance Test) were compared using parametric one-way ANOVA followed by Dunnett's post hoc test. Otherwise, the Mann-Whitney test or non-parametric Kruskal-Wallis ANOVA on ranks were used. Differences between the control and treatments were considered statistically significant at p-values ≤ 0.05, with asterisks (*) indicating the use of parametric tests and hash symbols (#) indicating the use of non-parametric tests.

3. Results and discussion

3.1. Expression of OATP1B1 and 1B3 in 3D Hepoid-HepaRG

As MC-LR-induced hepatotoxicity depends on its cellular uptake mediated by OATP1B1 and 1B3, expression levels of the respective OATP-encoding genes, *SLCO1B1* and *SLCO1B3*, were analyzed in Hepoid-HepaRG (Fig. 1A). In comparison to the 2D culture of differentiated HepaRG, the expression of OATP1B1 in Hepoid-HepaRG increased nearly 3-fold on day 5, and showed a statistically significant 7- to 9-fold upregulation on days 15 and 28 of the 3D culture. Expression of OATP1B3 increased to a lesser degree, going from approximately a 1.4-fold increase on day 5 to a 3-fold increase on day 28 of Hepoid-HepaRG culture, when compared to 2D HepaRG. The ratio of OATP1B1 to OATP1B3 mRNA levels increased from approximately 10 in the 2D culture to approximately 50 on days 15 and 28 (Fig. 1A). These changes observed at the transcriptional level were corroborated by immunofluorescence experiments, which demonstrated increased expression and proper membrane localization of the OATP1B1 protein in the 3D Hepoid-HepaRG cultures (Fig. 1B). Our results are consistent with prior research indicating enhanced OATP1B1/1B3 expression or function in 3D spheroid cultures of HepG2 (Roegner and Puschner, 2014) or HepaRG cells (Ulvestad et al., 2012) compared to 2D monolayer cultures. Correspondingly, the 3D architecture of Hepoid-HepaRG cultures, consisting of small spheroids of polarized hepatic cells with a hollow lumen, has previously been associated with improved and more stable expression of differentiation markers, such as membrane transporters NTCP, BSEP, or MRP2 (Rose et al., 2022). The enhanced OATP expression indicated that 3D Hepoid-HepaRG cultures could serve as a sensitive *in vitro* model for studying hepatotoxicants like MC-LR, as we evaluated next.

3.2. Effects of MC-LR on cell viability

With respect to increased OATP1B1/1B3 expression levels during Hepoid-HepaRG cultures, MC-LR effects on the viability of differentially-aged spheroids were evaluated. MC-LR induced concentration-dependent decrease in cell viability, with the effects depending on the specific exposure regime (Fig. 1C). In 4-d-old Hepoid-

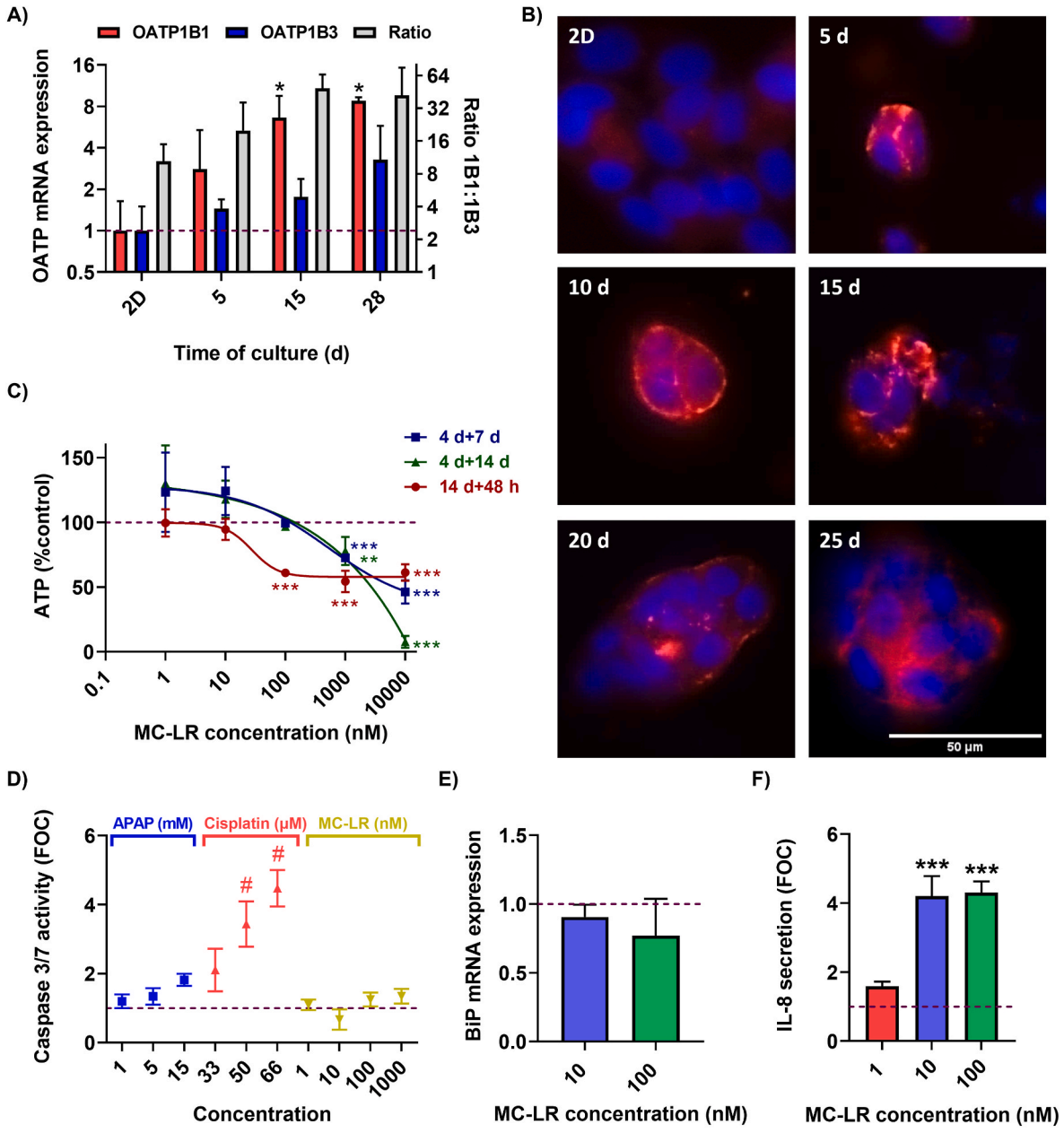

Fig. 1. Expression of OATP in Hepoid-HepaRG cultures and effects of microcystin-LR (MC-LR) on markers of cell viability, apoptosis, endoplasmic reticulum stress, and inflammation. (A) Fold change in OATP1B1 (*SLCO1B1*) and OATP1B3 (*SLCO1B3*) mRNA expression during 5-d, 15-d and 28-d culture of Hepoid-HepaRG relative to the 2D DMSO-differentiated HepaRG culture (left y-axis) and the gene expression ratio (right y-axis). (B) Immunofluorescence of OATP1B1 in 2D DMSO-differentiated HepaRG and 5-d, 10-d, 15-d and 25-d-old Hepoid-HepaRG cultures (red channel: OATP1B1, blue channel: nuclei, scale bar: 50 µm). (C) Cell viability evaluated by ATP assay in differentially matured (14 d or 4 d) Hepoid-HepaRG cultures in response to MC-LR exposures (48 h, 7 d or 14 d). 14-d-old Hepoid-HepaRG cultures and 48 h exposures to MC-LR were selected for subsequent experiments to evaluate: (D) apoptosis measured as caspase 3/7 activity, with Acetaminophen (APAP) or Cisplatin used as negative or positive chemical treatments; (E) fold change in mRNA expression of the endoplasmic reticulum stress marker gene BiP/GRP78 (*HSPA5*); (F) secretion of the inflammatory marker IL-8. Data represent mean ± SD of independently repeated experiments ($n \geq 3$), dashed reference line indicates the experimental control. Significant differences from the control were determined either by one-way ANOVA ($^{*}p \leq 0.05$, $^{**}p \leq 0.01$, $^{***}p \leq 0.001$) or Kruskal-Wallis ANOVA on ranks ($^{\#}p \leq 0.05$, $^{\#\#}p \leq 0.01$, $^{\#\#\#}p \leq 0.001$), depending on data normality and homogeneity of variance. (For interpretation of the references to color in this figure legend, the reader is referred to the Web version of this article.)

HepaRG cultures with a lower OATP expression, significant cytotoxic effects were observed at MC-LR concentrations of 1000 and 10000 nM after 7 or 14 d exposure (Fig. 1C). The effective concentrations (EC) were estimated as $EC_{20} = 537$ nM and $EC_{50} = 6572$ nM for the 7-d exposure, and $EC_{20} = 646$ nM and $EC_{50} = 2726$ nM for the 14-d exposure (Table S2). However, 14-d-old Hepoid-HepaRG, with higher OATP expression, were found to be more sensitive to MC-LR compared to less mature 4-d-old cultures. After 48-h exposure to concentrations >10 nM, Hepoid-HepaRG showed a significant decrease in ATP levels ($EC_{20} = 26$ nM, Table S2). Concentration 100 nM caused approximately 40% reduction in cell viability, accompanied by visible destruction of Hepoid-HepaRG spheroids (Fig. S1).

Previous studies with 2D differentiated HepaRG cells reported that 48-h exposures to 100–1000 nM MC-LR significantly reduced XTT-evaluated viability (Biales et al., 2020), with a 20% decrease caused by 1000 nM concentration (~EC_{20}) (Duan et al., 2018). Another study reported 15–45% decrease in MTT-evaluated viability of 2D HepaRG cultures exposed to 1–500 nM MC-LR for 72 h (Niture et al., 2023). The

14-d-old Hepoid-HepaRG cultures thus appear to be more sensitive to MC-LR than 2D differentiated HepaRG cells. MC-LR sensitivity of Hepoid-HepaRG is comparable to that of primary human cells, as reported EC_{50} values for PHH fall between 3.4 and 119 nM, with the lowest effective concentrations typically between 10 and 100 nM, depending on the duration of the exposure (6 h–48 h) or other experimental conditions (Batista et al., 2003; Fischer et al., 2010; Ikehara et al., 2015; Ufelmann et al., 2012; Woolbright et al., 2017). In contrast, conventional 2D cultures of immortalized hepatic cells usually require significantly higher MC-LR concentrations, exceeding 1000–10000 nM, to induce significant cytotoxic effects. This has been reported for monolayer cultures of HepG2 (Ikehara et al., 2015; Jasionek et al., 2010; Ma et al., 2017), Huh7 (Christen et al., 2013), HL7702 (Chen et al., 2012; Wang et al., 2023), or HL1-hT1 cells (Raska et al., 2018). Interestingly, similar to HepaRG cells, the sensitivity of these cell lines to lower MC-LR concentrations (10–100 nM) can be enhanced through 3D cultivation, as observed in studies with HepG2 cells (Roegner and Puschner, 2014) and human liver stem cells HL1-hT1 (Basu et al., 2018).

Since the use of 3D cultures of human liver cells in MC-LR research has been limited, our results with Hepoid-HepaRG further demonstrate the potential of 3D cultures for enhancing sensitivity and *in vivo* relevance of *in vitro* hepatotoxicity studies (Ingelman-Sundberg and Lauschke, 2022; Serras et al., 2021; Yang et al., 2021). The 3D Hepoid-HepaRG model offers several advantages, including the utilization of an immortal and commercially available human cell line that is extensively employed in toxicological research (Ingelman-Sundberg and Lauschke, 2022; Serras et al., 2021). In contrast to conventional 2D HepaRG cells, Hepoid-HepaRG cultures enhance hepatocyte differentiation and function without a need for a treatment with high and unphysiological concentrations of DMSO (Rose et al., 2022). This versatile and physiologically relevant *in vitro* system thus provided a sensitive experimental model to investigate mechanisms of hepatotoxicity in response to toxicologically relevant MC-LR concentrations. Based on the higher OATP expression and increased sensitivity to MC-LR cytotoxicity compared to less mature 3D cultures, 14-d-old Hepoid-HepaRG cultures were selected for the subsequent experiments, to further characterize effects of MC-LR on hepatic cell injury and markers of cellular stress, inflammation, hepatic differentiation and function, induced by the subcytotoxic (10 nM) and the lowest cytotoxic (100 nM) MC-LR concentrations.

3.3. Effects of MC-LR on markers of apoptosis, ER stress and inflammatory responses

Considering the cytotoxicity indicating a MC-LR-induced cell death, the caspase 3/7 activity was evaluated as a marker of apoptotic programmed cell death. No increase in caspase 3/7 activity was found at noncytotoxic/subcytotoxic (1–10 nM) as well as cytotoxic (100–1000 nM) concentrations of MC-LR, which resembled the response of necrosis-inducing acetaminophen rather than apoptosis-inducing cisplatin (Fig. 1D). Furthermore, 10–100 nM MC-LR did not significantly alter the expression levels of the ER stress marker gene *HSP5A* encoding the Heat Shock Protein 70 (HSP70), also known as Binding Immunoglobulin Protein (BiP)/GRP78 (Fig. 1E). Apoptosis has been frequently studied as a cell death mechanism in connection to MC-LR-induced oxidative stress, leading to ER stress and unfolded protein response (Shi et al., 2021). However, the lack of activation of caspases 3/7, major executioner caspases in apoptosis (Nirmala and Lopus, 2020) together with no effects on the expression of ER stress marker BiP/GRP78, known as an activator of apoptosis-related genes in response to MC-LR (Christen et al., 2013), suggests that apoptosis may not be the primary mechanism of cell death in the Hepoid-HepaRG model under the tested conditions. This observation is consistent with studies that reported MC-LR-induced rapid necrotic cell death in human hepatocytes without involving apoptosis (Woolbright et al., 2017), as well as the identification of alternative forms of programmed cell death caused by MC-LR, such as necroptosis (Wu et al., 2019).

Necrotic or necroptotic cell death is associated with inflammation (Nirmala and Lopus, 2020), and MC-LR *in vivo* and *in vitro* exposures have been linked to inflammatory responses (Kubickova et al., 2019; Shi et al., 2021). Correspondingly, we observed a significant increase in the secretion of the pro-inflammatory cytokine IL-8 by 10–100 nM MC-LR in the Hepoid-HepaRG model (Fig. 1F). Increased levels of IL-8 were previously observed in the liver of MC-LR-exposed mice (Chen et al., 2018). IL-8 can be produced by many cell types, including hepatocytes, and is known to attract neutrophil infiltration to the liver. Its release has been associated with various types of liver injury and chronic liver diseases (Wang et al., 2021). Chronic inflammation represents an important mechanism in HCC (Sun and Karin, 2013), with IL-8 involved in the regulation of proliferation, invasion, and metastasis of liver cancer cells (Bi et al., 2019; Ha et al., 2017; Sun et al., 2019).

In summary, submicromolar concentrations of MC-LR induced cytotoxic effects and disintegration of Hepoid-HepaRG spheroids, without involvement of the caspase-3/7-dependent apoptotic pathway or ER stress markers, while being associated with IL-8 release. Hence, future MC-LR studies should focus on inflammation-associated necrotic or necroptotic cell death, as a mechanism known to contribute to hepatocarcinogenesis (Bi et al., 2019; Ha et al., 2017; Sun and Karin, 2013; Sun et al., 2019; Wang et al., 2021).

3.4. Effects of MC-LR on hepatocyte functionality

Based on the evidence of hepatic cell injury caused by MC-LR in 14-d-old Hepoid-HepaRG cells, we evaluated its impact on major hepatocyte functions, including albumin secretion and expression, urea production, and activity and expression of phase I biotransformation enzymes. MC-LR reduced albumin secretion in a concentration-dependent manner, significantly decreasing to 50–60% at 10–100 nM (Fig. 2A). Correspondingly, exposure to 10 nM or 100 nM MC-LR downregulated albumin gene expression by 1.8-fold and 7-fold, respectively (Fig. 2B). However, urea secretion was not significantly affected (Fig. 2C). On the other hand, expression of a major phase I biotransformation enzyme, cytochrome P450 1A2 (*CYP1A2*), was reduced in response to 10–100 nM MC-LR by 8- to 33-fold (Fig. 2D). To assess the impact of MC-LR on xenobiotic metabolism phase I enzyme activity, EROD and MROD assays were performed. In the control cells or cells treated with 100 nM MC-LR alone, minimal or undetectable basal EROD/MROD activities were found (Table 1). EROD/MROD activity was induced in Hepoid-HepaRG when the cells were treated with 3-MC, a polycyclic aromatic hydrocarbon (Table 1). However, MC-LR exposures significantly impaired 3-MC-dependent EROD/MROD induction, reducing it to 25–35% of 3-MC-treated solvent control at 10 nM MC-LR and to <5% at 100 nM MC-LR (Table 1).

Clearly, both subcytotoxic and cytotoxic MC-LR concentrations had significant effects on crucial hepatocyte functionalities in Hepoid-HepaRG, impacting albumin secretion and phase I enzymes at both gene expression and functional levels. Similarly, reduced albumin secretion, gene expression and activity of cytochrome P450 were observed in MC-LR-exposed mice (Clark et al., 2007; Zhang et al., 2015). These results suggest that exposure to MC-LR may lead to a rapid loss of hepatic functions due to suppression of hepatocyte-specific genes and dedifferentiation of hepatic cells, and/or due to the elimination of the most differentiated cells from the population, Hence, we further evaluated expression of additional gene markers of hepatic differentiation.

3.5. Effects of MC-LR on OATP expression and other hepatocyte-differentiation gene markers

To evaluate the expression of genes associated with hepatocyte differentiation, we first examined the expression of genes encoding the key hepatobiliary membrane transporters, namely OATP1B1, OATP1B3, NTCP (*SLCO1B1*, *SLCO1B3*, *SLC10A1*, respectively) and BSEP

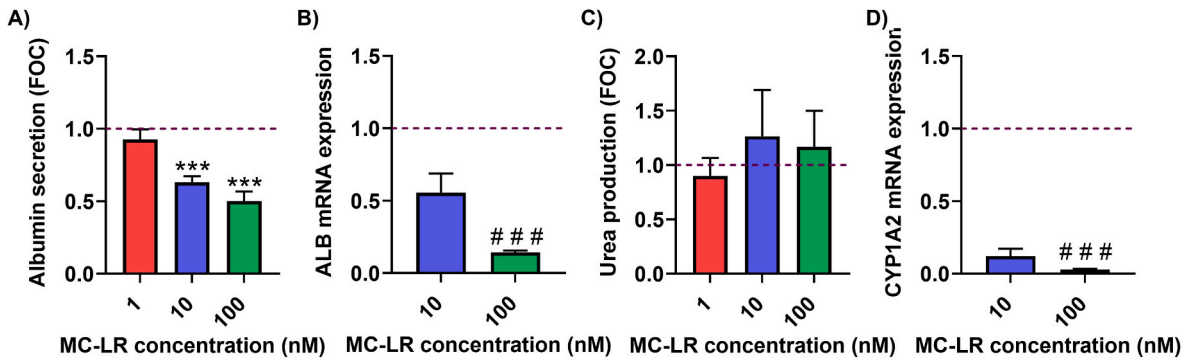

Fig. 2. Effects of microcystin-LR (MC-LR) on hepatic cell functionality in Hepoid-HepaRG cultures. 14-d-old Hepoid-HepaRG cultures were exposed to MC-LR for 48 h to evaluate: (A) albumin concentration in the culture medium; (B) fold change in mRNA expression of albumin gene (*ALB*); (C) urea concentration in the culture medium; and (D) mRNA expression of CYP1A2 gene (*CYP1A2*). Data represent mean ± SD of independently repeated experiments (n ≥ 3), dashed reference line indicates the solvent control. Significant differences from the solvent control were determined either by one-way ANOVA (*p ≤ 0.05, **p ≤ 0.01, ***p ≤ 0.001) or Kruskal-Wallis ANOVA on ranks ($^{\#}$p ≤ 0.05, $^{\#\#}$p ≤ 0.01, $^{\#\#\#}$p ≤ 0.001), depending on data normality and homogeneity of variance.

Table 1
Effects of microcystin-LR (MC-LR) on phase I enzyme activity in Hepoid-HepaRG.

Treatment	EROD (% of 3-MC-induced control)		MROD (% of 3-MC-induced control)	
	Basal	**3-MC**	**Basal**	**3-MC**
Solvent control	0.1 ± 0.3%	100 ± 0.0%	<LOD	100 ± 0.0%
10 nM MC-LR	n.a.	34.7 ± 3.8% ***	n.a.	25.4 ± 13.8%
100 nM MC-LR	0.1 ± 0.2%	4.6 ± 1.9% ***	<LOD	0.3 ± 0.5% #

14-d-old Hepoid-HepaRG cultures were exposed to microcystin-LR (MC-LR) for 48 h. The measurement of cytochrome P450 activity by EROD or MROD assay was done either without (basal) or with 3-methylcholantrene (3-MC) treatment. 3-MC was added to the cultures 24 h after the initiation of MC-LR treatment, i.e. 24 h prior to the assay. Cell viability-normalized activities were expressed as percentage of 3-MC-induced solvent control. Data represent mean ± SD of three independently repeated experiments. Significant differences from the solvent control were determined either by one-way ANOVA (*p ≤ 0.05, **p ≤ 0.01, ***p ≤ 0.001) or Kruskal-Wallis ANOVA on ranks (#p ≤ 0.05, ##p ≤ 0.01, ###p ≤ 0.001), depending on data normality and homogeneity of variance.

(*ABCB11*). OATP1B1 expression was significantly downregulated at both 10 nM and 100 nM MC-LR concentrations, showing approximately a 3-fold and 20-fold reduction compared to the control, respectively (Fig. 3A). In contrast, OATP1B3 expression exhibited an increasing trend in response to MC-LR, with 100 nM causing a significant 2.5-fold induction. Similarly to OATP1B1, the gene expression levels of NTCP and BSEP were significantly downregulated by both MC-LR concentrations (Fig. 3A). The substantial decrease in the expression of dominant OATP1B1 (Fig. 1A), coupled with comparably smaller increase of less expressed OATP1B3, led to a significant shift in the ratio of the two genes. The OATP1B1:1B3 ratio, which was around 50 in the control cells, thus became equalized in the cells treated with 100 nM of MC-LR, which indicates a significant reduction in the combined expression of OATP1B1 and 1B3 (Fig. 3E). The reduced expression of OATPs may contribute to a decrease in cell sensitivity to MC-LR, as previously reported in PHH cultures with different levels of OATP1B1 expression (Ikehara et al., 2015). This could explain the plateauing of cytotoxic effects at around 55–60% of the control after 48-h MC-LR exposure in the mature Hepoid-HepaRG cultures. In these cultures, the most differentiated hepatocytes highly expressing OATPs would be susceptible to toxin uptake and consequent cytotoxicity and rapid cell death. In contrast, lower OATP expression in less mature and less differentiated cells may confer their resilience to MC-LR-induced cytotoxicity in the short-term exposures. However, the progressing differentiation (Fig. 1A–B) during longer 7-d or 14-d exposures of less mature Hepoid-HepaRG cells resulted in almost complete loss of viable cells at higher MC-LR concentrations (Fig. 1C).

Next, we analyzed the effects of MC-LR on the expression of genes associated with hepatocyte differentiation and implicated in hepatocarcinogenesis. MC-LR caused significant downregulation of the gene encoding adherens junction protein and epithelial cell marker E-cadherin (*CDH1*). Its expression was significantly reduced by approximately 2-fold and 8-fold in response to 10 nM and 100 nM MC-LR, respectively (Fig. 3B). In contrast, the expression levels of the gene encoding a mesenchymal cell marker N-cadherin (*CDH2*) were affected to a lesser extent. A significant reduction of N-cadherin expression to approximately 60% of the control was observed only at 100 nM MC-LR (Fig. 3B). Consequently, the initial E:N-cadherin ratio, which was approximately 1.5 in the control Hepoid-HepaRG, showed a statistically significant switch to N:E-cadherin ratio ranging between 1.3 and 3.4 (Fig. 3E). MC-LR treatment also caused a significant downregulation of hepatocyte nuclear factor 4 α gene (*HNF4A*) at both tested concentrations, while it did not significantly affect the expression of the alpha-fetoprotein gene (*AFP*) (Fig. 3C). Concomitantly, the expression of the gap junctional protein connexin 32 (Cx32), encoded by the *GJB1* gene, was significantly downregulated by 2- to 8-fold in response to 10 and 100 nM MC-LR, respectively (Fig. 3D). In contrast, the expression levels of connexin 43 (Cx43), encoded by the *GJA1* gene, increased approximately 1.5-fold in response to MC-LR treatment. This caused a significant shift in the Cx32:Cx43 ratio, from approximately 8 in the control to <1 in the cells treated with 100 nM MC-LR (Fig. 3E).

Overall, the treatment of Hepoid-HepaRG cultures with 10–100 nM MC-LR decreased expression of key markers of differentiated hepatocytes, including genes for OATP1B1, NTCP, BSEP, E-cadherin, HNF4α and Cx32, as well as albumin and CYP1A2. Conversely, gene markers associated with immature or non-parenchymal cells or with diseased states, such as OATP1B3, N-cadherin, AFP, and Cx43, were less affected or exhibited increased expression.

OATP1B1/1B3, NTCP and BSEP are membrane transporters that are localized in the opposite regions of polarized hepatocytes, with OATP1B1/1B3 and NTCP localized on the sinusoidal side while BSEP is present on the canalicular side (Durník et al., 2022). The significant downregulation in the expression levels of OATP1B1, NTCP and BSEP in MC-LR treated Hepoid-HepaRG cultures thus suggests a progressive loss of the phenotype of differentiated polarized hepatocytes. Dysregulations of hepatobiliary transporters, including OATP1B1/1B3, NTCP and BSEP, have been implicated in the pathogenesis of inflammatory liver injuries, cholestasis, fatty liver disease, liver cirrhosis, and liver cancer (Halilbasic et al., 2013; Taniguchi et al., 2020; Thakkar et al., 2017). Reduced expression of Ntcp, Oatp1a4 and Oatp1b2 (a rodent equivalent of OATP1B1/1B3) following prolonged sublethal exposures of mice to MC-LR was associated with preneoplastic hepatic lesions (Clark et al.,

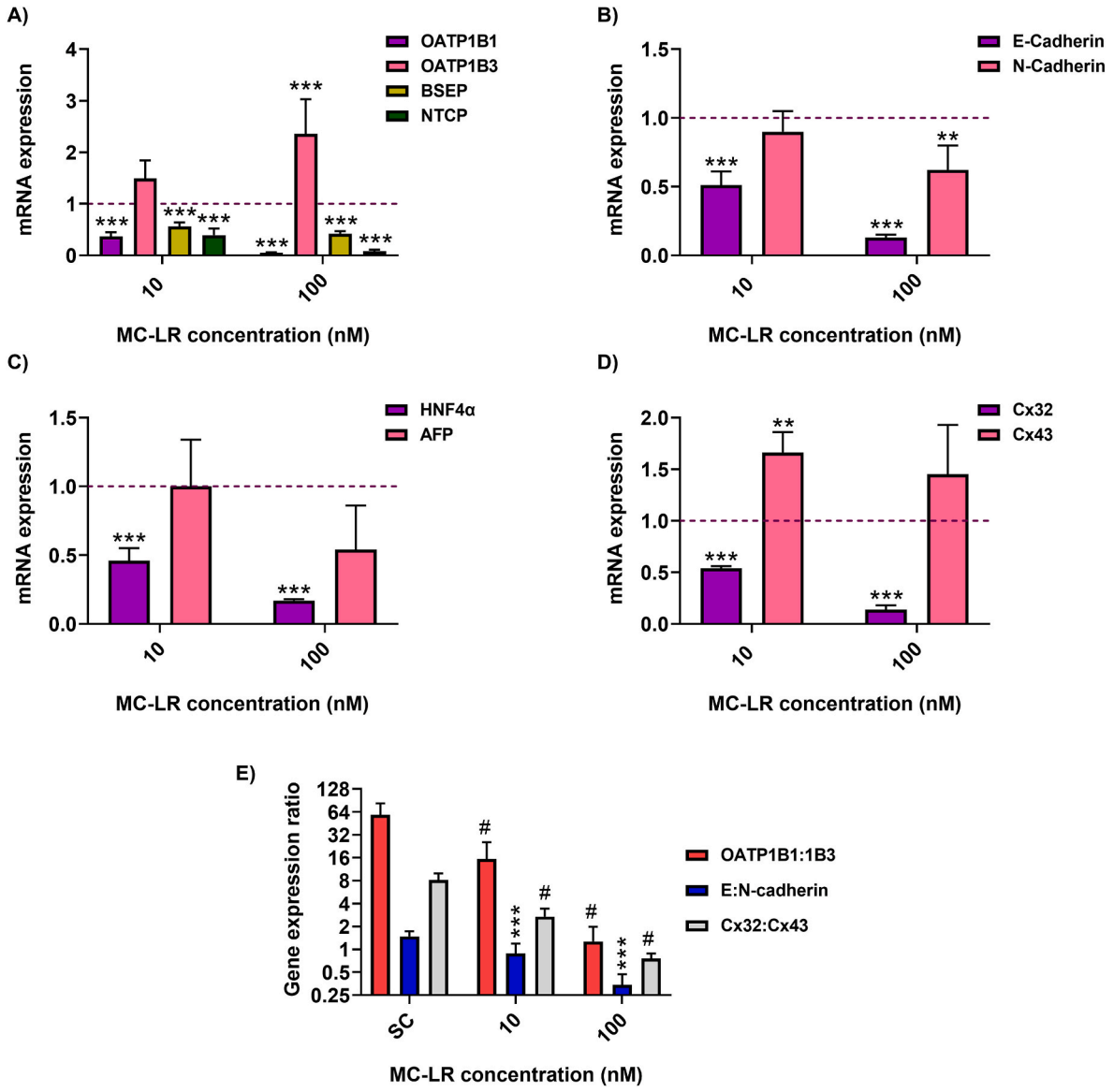

Fig. 3. Effects of microcystin-LR (MC-LR) on hepatocyte-differentiation markers in Hepoid-HepaRG cultures. 14-d-old Hepoid-HepaRG cultures were exposed to MC-LR for 48 h to evaluate fold change in mRNA expression of: (A) sinusoidal membrane transporters genes OATP1B1 (*SLCO1B1*), OATP1B3 (SLCO1B3) and NTCP (*SLC10A1*), and a canalicular membrane transporter gene BSEP (*ABCB11*); (B) adherens junction genes E-Cadherin (*CDH1*, an epithelial cell marker) and N-Cadherin (*CDH2*, a mesenchymal cell marker), (C) marker genes of hepatocyte differentiation HNF4α and AFP (*HNF4A* and *AFP*); and (D) gap junction genes connexin 32, Cx32 (*GJB1*, a differentiated hepatocyte marker) and connexin 43, Cx43 (*GJA1*, a marker of progenitor and nonparenchymal cells). (E) Expression ratios of selected gene pairs. Data represent mean ± SD of independently repeated experiments ($n \geq 3$), and dashed reference lines indicate the solvent control (SC). Significant differences from the solvent control were determined either by one-way ANOVA ($^{*}p \leq 0.05$, $^{**}p \leq 0.01$, $^{***}p \leq 0.001$) or Kruskal-Wallis ANOVA on ranks ($^{\#}p \leq 0.05$, $^{\#\#}p \leq 0.01$, $^{\#\#\#}p \leq 0.001$), depending on data normality and homogeneity of variance.

2007). Upregulation of a short cancer-specific type OATP1B3 (Ct-OATP1B3) has been detected in certain colon and lung tumors, but the full-length, liver-type OATP1B3 appears to be the predominant form in HCC (Anabtawi et al., 2022). While OATP1B3 expression is typically downregulated in HCC, its increased expression has been linked to a specific subclass of HCC associated with Wnt/β-catenin activation (Khalaf et al., 2018). In fact, Wnt/β-catenin pathway has been implicated in MC-LR-induced hepatocarcinogenesis *in vitro* and *in vivo* (Chen et al., 2019). On the other hand, expression of AFP, a marker of hepatoblasts, hepatic progenitor cells and immature/fetal hepatocytes (Kuhlmann and Peschke, 2006) was not significantly altered in the Hepoid-HepaRG model, which suggests that the less differentiated cells with low OATP expression were not primarily targeted by MC-LR.

The alteration of hepatocyte differentiation in Hepoid-HepaRG cells by MC-LR was also reflected in the expression of genes encoding gap junctional proteins, namely Cx32 and Cx43. Connexins play a critical role in maintaining liver tissue homeostasis by regulating various cellular functions, including cell functions, proliferation, differentiation and apoptosis (Hernández-Guerra et al., 2019; Trosko, 2021; Willebrords et al., 2016). Downregulation of Cx32, primarily expressed by differentiated hepatocytes (Hernández-Guerra et al., 2019; Willebrords et al., 2016), and upregulated expression of Cx43, expressed by hepatic progenitors and non-parenchymal cells, caused a significant shift in the Cx32:Cx43 expression ratio towards Cx43, It indicates disruption of tissue homeostasis and represents a pattern associated with the progression of liver pathologies, including acute liver injury and chronic liver diseases such as cholestasis, fatty liver disease, fibrosis, cirrhosis and HCC (Hernández-Guerra et al., 2019; Trosko, 2021; Willebrords et al., 2016).

Correspondingly to these changes in gene expression, MC-LR

downregulated HNF4α, a key transcription factor that controls hepatic differentiation and the expression of most hepatocyte-specific genes (Babeu, 2014; Berasain et al., 2023; Walesky and Apte, 2015). Additionally, HNF4α plays a role in suppressing oncogenic and inflammatory genes. Repression of HNF4α results in hepatocyte dedifferentiation, loss of the epithelial polarized phenotype, increased proliferation, induction of epithelial-mesenchymal transition (EMT) and faster progression of HCC (Babeu, 2014; Berasain et al., 2023; Walesky and Apte, 2015). EMT is an important phenomenon during tumor progression, where the tumor cells of epithelial origin acquire characteristics of mesenchymal-like cells, which increases their motility, apoptosis resistance, invasiveness and metastatic activity (Loh et al., 2019; Ribatti et al., 2020). This process is hallmarked by the downregulation of adherens junctions protein E-cadherin and other epithelial markers, accompanied by increased expression of mesenchymal markers, such as N-cadherin (Loh et al., 2019; Ribatti et al., 2020). In Hepoid-HepaRG cells, MC-LR significantly reduced the expression of E-cadherin, while its effects on the expression of N-cadherin were much less pronounced. As a result, there was a change in the E:N-cadherin expression ratio, shifting significantly towards N-cadherin. Previously, MC-LR has been shown to promote EMT in HEK293-OATP1B3 cells that survived MC-LR-induced anoikis (Takano et al., 2014), in colorectal cancer cells (Ren et al., 2017), and also in *in vivo* and *in vitro* models of prostate cancer (Pan et al., 2023). Furthermore, environmental exposures to MC-LR have been associated with the promotion of EMT in prostate cancer patients (Pan et al., 2023).

3.6. Mechanistic implications and toxicological relevance

Taken together, exposures of Hepoid-HepaRG cultures to 10–100 nM MC-LR resulted in liver cell injury, a pro-inflammatory cytokine release, loss of major hepatocyte functions and alterations of key hepatocyte genes (Fig. 4). MC-LR caused progressive loss of hepatocyte differentiation, disruption of liver tissue homeostasis and induction of EMT markers, events known to contribute to the promotion and progression of HCC. While some of these events have been implicated in MC-LR mode of action previously, this study demonstrates their comprehensive manifestation for the first time in a 3D *in vitro* human liver model. This mechanistic evidence further supports the existing experimental and epidemiological studies on the ability of MC-LR to contribute to the development of chronic liver diseases, including tumor-promoting and hepatocarcinogenic effects (Buratti et al., 2017; Shi et al., 2021; Svirčev et al., 2019).

Importantly, the concentrations of MC-LR that were effective in the Hepoid-HepaRG model are toxicologically relevant. Prolonged (28 d) repeated exposures of rodents to nonlethal doses of MC-LR resulted in toxin plasma concentrations 5 ng/mL (~5 nM) and liver concentrations 142–2000 ng/g (Sedan et al., 2013; Solter et al., 1998), which corresponds to ~150–2113 nM (assuming a liver density of 1.05 g/mL, Overmoyer et al., 1987). Serum microcystin levels in acute human poisonings ranged from 0.2 to 29 ng/mL (~0.2–29 nM) (Hilborn and Beasley, 2015), while liver tissue concentrations in fatal or liver transplant-requiring cases were around 78–223 ng/g (~82–236 nM) (Azevedo et al., 2002; Vidal et al., 2017, p. 20). In chronically exposed human populations, microcystin concentrations in the serum ranged from 0.1 to 5 ng/mL (~0.1–5 nM), with higher concentrations being associated with hepatocellular damage, impaired insulin levels and increased risks of HCC (Chen et al., 2009; He et al., 2018; Hernandez et al., 2023; Li et al., 2011; Zhao et al., 2016; Zheng et al., 2017). Our previous study confirmed that analytically measured MC-LR concentrations in a 3D *in vitro* human liver model corresponded to the nominal toxin concentrations, with no significant changes due to sorption, degradation, or evaporation observed even during 14-d exposures (Basu et al., 2018). The Hepoid-HepaRG model proved to be a relevant tool for microcystin effects at concentrations reflecting real-life exposures. This *in vitro* model is well-suited for extended exposures lasting several days or weeks (Rose et al., 2022), making it ideal for studying the effects of low MC-LR concentrations found in plasma of chronically exposed

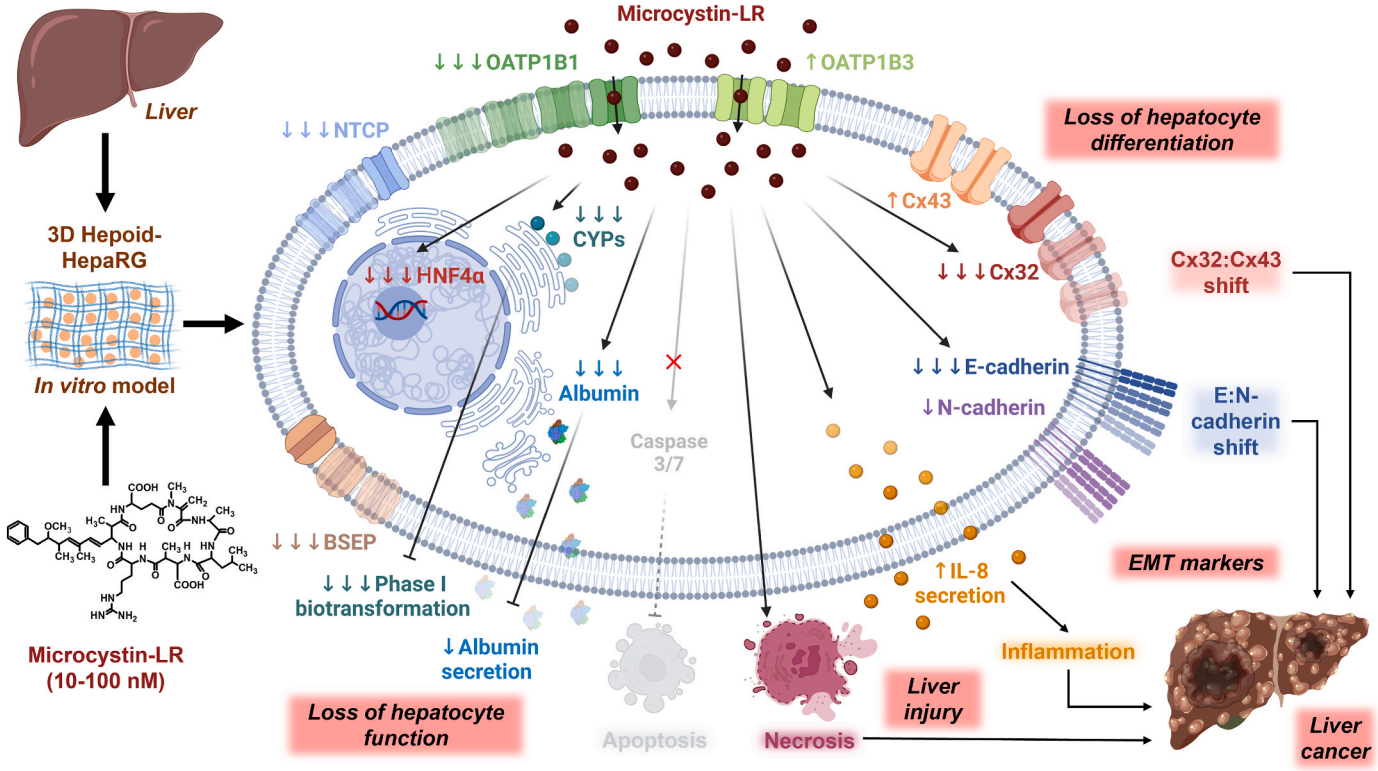

Fig. 4. Overview of microcystin-LR effects induced in 3D Hepoid-HepaRG cultures.
Created with BioRender.com.

human populations. It offers a versatile system that can be combined with a variety of assays and endpoints (Rose et al., 2022), thus enabling future in-depth investigations into the mechanisms underlying MC-LR-induced chronic liver toxicity, including genotoxicity, oxidative stress, inflammation, metabolic disruption or epigenetic toxicity, and their role in the development of chronic liver diseases, such as HCC.

4. Conclusion

3D Hepoid-HepaRG cultures represent *in vitro* model of the human liver based on a well-characterized and widely used cell line. This model is highly sensitive in detecting the effects of MC-LR, an environmental hepatotoxin predominantly targeting well-differentiated hepatocyte cells. By using Hepoid-HepaRG, we were able to investigate responses of human liver cells to toxicologically relevant concentrations and identify major mechanisms potentially contributing to MC-LR hepatocarcinogenic activity. The application of advanced 3D *in vitro* models represents a significant improvement in studying the hazardous effects of microcystins and contributes to assessing their risks to human health.

Author statement

Riju R. Chowdhury: Conceptualization, Data curation, Formal analysis, Funding acquisition, Investigation, Methodology, Project administration, Validation, Visualization, Writing - original draft, Writing - review & editing, Sophie Rose: Investigation, Methodology, Supervision, Validation, Writing - review & editing, Frédéric Ezan: Investigation, Methodology, Validation, Writing - review & editing, Iva Sovadinová: Formal analysis, Methodology, Validation, Writing - review & editing, Pavel Babica: Conceptualization, Formal analysis, Funding acquisition, Methodology, Resources, Supervision, Visualization, Writing - original draft, Writing - review & editing, Sophie Langouët: Conceptualization, Funding acquisition, Methodology, Project administration, Resources, Supervision, Writing - original draft, Writing - review & editing.

Funding

The study was funded by the Czech Science Foundation (GAČR) – project no. GA19-19143S. Authors thank the Research Infrastructure RECETOX RI (LM2023069) financed by the Ministry of Education, Youth and Sports, and Operational Programme Research, Development, and Education—project CETOCOEN EXCELLENCE (CZ.02.1.01/0.0/0.0/17_043/0009632), for supportive background. This work was supported by the European Union's Horizon 2020 research and innovation programme under grant agreement No. 857560—CETOCOEN Excellence. This publication reflects only the author's view and the European Commission is not responsible for any use that may be made of the information it contains*T*. Mobility of R. R. Chowdhury was supported by the Barrande Fellowship Programme funded by The French Institute in Prague and the Czech Ministry of Education, Youth and Sports. The authors thank the platform H2P2 from the SFR Biosit (UMS CNRS 3480/US INSERM 018, Biogenouest, University of Rennes). This work was also supported by the Institut National de la Santé et de la Recherche Médicale (Inserm), the University of Rennes and the European Digital UniverCity EDUC. EDUC-Share project funded by the European Union's Horizon 2020 research and innovation programme under grant agreement No. 101017526 is also gratefully acknowledged for encouraging collaboration between Rennes and Masaryk Universities.

Declaration of competing interest

The authors declare that they have no known competing financial interests or personal relationships that could have appeared to influence the work reported in this paper.

Data availability

Data will be made available on request.

Appendix A. Supplementary data

Supplementary data to this article can be found online at https://doi.org/10.1016/j.envpol.2023.123047.

References

Anabtawi, N., Drabison, T., Hu, S., Sparreboom, A., Talebi, Z., 2022. The role of OATP1B1 and OATP1B3 transporter polymorphisms in drug disposition and response to anticancer drugs: a review of the recent literature. Expet Opin. Drug Metabol. Toxicol. 18, 459–468. https://doi.org/10.1080/17425255.2022.2113380.

Azevedo, S.M.F.O., Carmichael, W.W., Jochimsen, E.M., Rinehart, K.L., Lau, S., Shaw, G. R., Eaglesham, G.K., 2002. Human intoxication by microcystins during renal dialysis treatment in Caruaru–Brazil. Toxicology 181–182, 441–446. https://doi.org/10.1016/S0300-483X(02)00491-2.

Babeu, J.-P., 2014. Hepatocyte nuclear factor 4-alpha involvement in liver and intestinal inflammatory networks. World J. Gastroenterol. 20, 22. https://doi.org/10.3748/wjg.v20.i1.22.

Basu, A., Dydowiczová, A., Čtveráčková, L., Jaša, L., Trosko, J.E., Bláha, L., Babica, P., 2018. Assessment of hepatotoxic potential of cyanobacterial toxins using 3D in vitro model of adult human liver stem cells. Environ. Sci. Technol. 52, 10078–10088. https://doi.org/10.1021/acs.est.8b02291.

Batista, T., de Sousa, G., Suput, J.S., Rahmani, R., Suput, D.A., 2003. Microcystin-LR causes the collapse of actin filaments in primary human hepatocytes. Aquat. Toxicol. 65, 85–91. https://doi.org/10.1016/s0166-445x(03)00108-5.

Battle, T., Maguire, T., Moulsdale, H., Doyle, A., 1999. Progressive maturation resistance to microcystin-LR cytotoxicity in two different hepatospheroidal models. Cell Biol. Toxicol. 15, 3–12. https://doi.org/10.1023/a:1007587304619.

Berasain, C., Arechederra, M., Argemí, J., Fernández-Barrena, M.G., Avila, M.A., 2023. Loss of liver function in chronic liver disease: an identity crisis. J. Hepatol. 78, 401–414. https://doi.org/10.1016/j.jhep.2022.09.001.

Bi, H., Zhang, Y., Wang, S., Fang, W., He, W., Yin, L., Xue, Y., Cheng, Z., Yang, M., Shen, J., 2019. Interleukin-8 promotes cell migration via CXCR1 and CXCR2 in liver cancer. Oncol. Lett. https://doi.org/10.3892/ol.2019.10735.

Biales, A.D., Bencic, D.C., Flick, R.W., Delacruz, A., Gordon, D.A., Huang, W., 2020. Global transcriptomic profiling of microcystin-LR or -RR treated hepatocytes (HepaRG). Toxicon X 8, 100060. https://doi.org/10.1016/j.toxcx.2020.100060.

Bomo, J., Ezan, F., Tiaho, F., Bellamri, M., Langouët, S., Theret, N., Baffet, G., 2016. Increasing 3D matrix rigidity strengthens proliferation and spheroid development of human liver cells in a constant growth factor environment. J. Cell. Biochem. 117, 708–720. https://doi.org/10.1002/jcb.25356.

Buratti, F.M., Manganelli, M., Vichi, S., Stefanelli, M., Scardala, S., Testai, E., Funari, E., 2017. Cyanotoxins: producing organisms, occurrence, toxicity, mechanism of action and human health toxicological risk evaluation. Arch. Toxicol. 91, 1049–1130. https://doi.org/10.1007/s00204-016-1913-6.

Chen, D. ni, Zeng, J., Wang, F., Zheng, W., Tu, W. wei, Zhao, J., shun Xu, J., 2012. Hyperphosphorylation of intermediate filament proteins is involved in microcystin-LR-induced toxicity in HL7702 cells. Toxicol. Lett. 214, 192–199. https://doi.org/10.1016/j.toxlet.2012.08.024.

Chen, H., Zhao, J., Li, Y., Huang, Y., Chen, D., He, L., Wang, L., Zheng, C., Wang, J., Cao, J., Shu, W., Liu, J., Liu, W., 2019. Epigenetic inactivation of LHX6 mediated microcystin-LR induced hepatocarcinogenesis via the Wnt/β-catenin and P53 signaling pathways. Environ. Pollut. 252, 216–226. https://doi.org/10.1016/j.envpol.2019.05.049.

Chen, J., Xie, P., Li, L., Xu, J., 2009. First identification of the hepatotoxic microcystins in the serum of a chronically exposed human population together with iindication of hepatocellular damage. Toxicol. Sci. 108, 81–89. https://doi.org/10.1093/toxsci/kfp009.

Chen, L., Liu, X., Pan, Z., Liu, S., Han, H., Zhao, C., Tang, X., 2018. The role of IL-8/CXCR2 signaling in microcystin-LR triggered endothelial cell activation and increased vascular permeability. Chemosphere 194, 43–48. https://doi.org/10.1016/j.chemosphere.2017.11.120.

Christen, V., Meili, N., Fent, K., 2013. Microcystin-LR induces endoplasmatic reticulum stress and leads to induction of NFκB, interferon-alpha, and tumor necrosis factor-alpha. Environ. Sci. Technol. 47, 3378–3385. https://doi.org/10.1021/es304886y.

Clark, S.P., Davis, M.A., Ryan, T.P., Searfoss, G.H., Hooser, S.B., 2007. Hepatic gene expression changes in mice associated with prolonged sublethal microcystin exposure. Toxicol. Pathol. 35, 594–605.

Duan, X., Sanan, T., de la Cruz, A., He, X., Kong, M., Dionysiou, D.D., 2018. Susceptibility of the algal toxin microcystin-LR to UV/chlorine process: comparison with chlorination. Environ. Sci. Technol. 52, 8252–8262. https://doi.org/10.1021/acs.est.8b00034.

Durník, R., Šindlerová, L., Babica, P., Jurček, O., 2022. Bile acids transporters of enterohepatic circulation for targeted drug delivery. Molecules 27, 1–24. https://doi.org/10.3390/molecules27092961.

Fischer, A., Hoeger, S.J., Stemmer, K., Feurstein, D.J., Knobeloch, D., Nussler, A., Dietrich, D.R., 2010. The role of organic anion transporting polypeptides (OATPs/SLCOs) in the toxicity of different microcystin congeners in vitro : a comparison of

primary human hepatocytes and OATP-transfected HEK293 cells. Toxicol. Appl. Pharmacol. 245, 9–20. https://doi.org/10.1016/j.taap.2010.02.006.
Fischer, W.J., Altheimer, S., Cattori, V., Meier, P.J., Dietrich, D.R., Hagenbuch, B., 2005. Organic anion transporting polypeptides expressed in liver and brain mediate uptake of microcystin. Toxicol. Appl. Pharmacol. 203, 257–263. https://doi.org/10.1016/j.taap.2004.08.012.
Gripon, P., Rumin, S., Urban, S., Le Seyec, J., Glaise, D., Cannie, I., Guyomard, C., Lucas, J., Trepo, C., Guguen-Guillouzo, C., 2002. Infection of a human hepatoma cell line by hepatitis B virus. Proc. Natl. Acad. Sci. U.S.A. 99, 15655–15660. https://doi.org/10.1073/pnas.232137699.
Ha, H., Debnath, B., Neamati, N., 2017. Role of the CXCL8-CXCR1/2 Axis in cancer and inflammatory diseases. Theranostics 7, 1543–1588. https://doi.org/10.7150/thno.15625.
Halilbasic, E., Claudel, T., Trauner, M., 2013. Bile acid transporters and regulatory nuclear receptors in the liver and beyond. J. Hepatol. 58, 155–168. https://doi.org/10.1016/j.jhep.2012.08.002.
He, L., Huang, Y., Guo, Q., Zeng, H., Zheng, C., Wang, J., Chen, J., Wang, L., Shu, W., 2018. Chronic Microcystin-LR exposure induces hepatocarcinogenesis via increased gankyrin in vitro and in vivo. Cell. Physiol. Biochem. 49, 1420–1430. https://doi.org/10.1159/000493446.
Hernandez, B.Y., Zhu, X., Nagata, M., Loo, L., Chan, O., Wong, L.L., 2023. Cyanotoxin exposure and hepatocellular carcinoma. Toxicology 487, 153470. https://doi.org/10.1016/j.tox.2023.153470.
Hernández-Guerra, M., Hadjihambi, A., Jalan, R., 2019. Gap junctions in liver disease: implications for pathogenesis and therapy. J. Hepatol. 70, 759–772. https://doi.org/10.1016/j.jhep.2018.12.023.
Hilborn, E.D., Beasley, V.R., 2015. One health and cyanobacteria in freshwater systems: animal illnesses and deaths are sentinel events for human health risks. Toxins 7, 1374–1395. https://doi.org/10.3390/toxins7041374.
IARC, 2010. IARC monographs on the evaluation of carcinogenic risks to humans. Ingested nitrate and nitrite, and cyanobacterial peptide toxins. IARC Monogr. Eval. Carcinog. Risks Hum. 94, 1–412.
Ikehara, T., Nakashima, J., Nakashima, S., Yasumoto, T., 2015. Different responses of primary normal human hepatocytes and human hepatoma cells toward cyanobacterial hepatotoxin microcystin-LR. Toxicon 105, 4–9. https://doi.org/10.1016/j.toxicon.2015.08.025.
Ingelman-Sundberg, M., Lauschke, V.M., 2022. 3D human liver spheroids for translational pharmacology and toxicology. Basic Clin. Pharmacol. Toxicol. 130, 5–15. https://doi.org/10.1111/bcpt.13587.
Jasionek, G., Zhdanov, A., Davenport, J., Blaha, L., Papkovsky, D.B., 2010. Mitochondrial toxicity of microcystin-LR on cultured cells: application to the analysis of contaminated water samples. Environ. Sci. Technol. 44, 2535–2541. https://doi.org/10.1021/es903157h.
Khalaf, A.M., Fuentes, D., Morshid, A.I., Burke, M.R., Kaseb, A.O., Hassan, M., Hazle, J. D., Elsayes, K.M., 2018. Role of Wnt/β-catenin signaling in hepatocellular carcinoma, pathogenesis, and clinical significance. J. Hepatocell. Carcinoma 5, 61–73. https://doi.org/10.2147/jhc.s156701.
Kotani, N., Maeda, K., Debori, Y., Camus, S., Li, R., Chesne, C., Sugiyama, Y., 2012. Expression and transport function of drug uptake transporters in differentiated HepaRG Cells. Mol. Pharm. 9, 3434–3441. https://doi.org/10.1021/mp300171p.
Kubickova, B., Babica, P., Hilscherová, K., Šindlerová, L., 2019. Effects of cyanobacterial toxins on the human gastrointestinal tract and the mucosal innate immune system. Environ. Sci. Eur. 31 https://doi.org/10.1186/s12302-019-0212-2.
Kuhlmann, W.D., Peschke, P., 2006. Hepatic progenitor cells, stem cells, and AFP expression in models of liver injury: progenitor cells, stem cells and the biliary epithelium. Int. J. Exp. Pathol. 87, 343–359. https://doi.org/10.1111/j.1365-2613.2006.00485.x.
Lad, A., Breidenbach, J.D., Su, R.C., Murray, J., Kuang, R., Mascarenhas, A., Najjar, J., Patel, S., Hegde, P., Youssef, M., Breuler, J., Kleinhenz, A.L., Ault, A.P., Westrick, J. A., Modyanov, N.N., Kennedy, D.J., Haller, S.T., 2022. As we drink and breathe: adverse health effects of microcystins and other harmful algal bloom toxins in the liver, gut, lungs and beyond. Life 12, 418. https://doi.org/10.3390/life12030418.
Li, Y., Chen, J., Zhao, Q., Pu, C., Qiu, Z., Zhang, R., Shu, W., 2011. A cross-sectional investigation of chronic exposure to microcystin in relationship to childhood liver damage in the Three Gorges Reservoir Region, China. Environ. Health Perspect. 119, 1483–1488. https://doi.org/10.1289/ehp.1002412.
Loh, C.-Y., Chai, J.Y., Tang, T.F., Wong, W.F., Sethi, G., Shanmugam, M.K., Chong, P.P., Looi, C.Y., 2019. The E-Cadherin and N-Cadherin switch in epithelial-to-mesenchymal transition: signaling, therapeutic implications, and challenges. Cells 8, 1118. https://doi.org/10.3390/cells8101118.
Ma, J., Feng, Y., Jiang, S., Li, X., 2017. Altered cellular metabolism of HepG2 cells caused by microcystin-LR. Environ. Pollut. 225, 610–619. https://doi.org/10.1016/j.envpol.2017.03.029.
Nirmala, J.G., Lopus, M., 2020. Cell death mechanisms in eukaryotes. Cell Biol. Toxicol. 36, 145–164. https://doi.org/10.1007/s10565-019-09496-2.
Niture, S., Gadi, S., Qi, Q., Rios-Colon, L., Khatiwada, S., Vandana Fernando, R.A., Levine, K.E., Kumar, D., 2023. Cyanotoxins increase cytotoxicity and promote nonalcoholic fatty liver disease progression by enhancing cell steatosis. Toxins 15, 411. https://doi.org/10.3390/toxins15070411.
Overmoyer, B.A., McLaren, C.E., Brittenham, G.M., 1987. Uniformity of liver density and nonheme (storage) iron distribution. Arch. Pathol. Lab Med. 111, 549–554.
Pan, C., Qin, H., Yan, M., Qiu, X., Gong, W., Luo, W., Guo, H., Han, X., 2023. Environmental microcystin exposure triggers the poor prognosis of prostate cancer: evidence from case-control, animal, and in vitro studies. J. Environ. Sci. 127, 69–81. https://doi.org/10.1016/j.jes.2022.05.051.
Plaas, H.E., Paerl, H.W., 2021. Toxic cyanobacteria: a growing threat to water and air quality. Environ. Sci. Technol. 55, 44–64. https://doi.org/10.1021/acs.est.0c06653.
Raska, J., Ctverackova, L., Dydowiczova, A., Sovadinova, I., Blaha, L., Babica, P., 2018. Tumor-promoting cyanotoxin microcystin-LR does not induce procarcinogenic events in adult human liver stem cells. Toxicol. Appl. Pharmacol. 345, 103–113. https://doi.org/10.1016/j.taap.2018.03.011.
Ren, Y., Yang, M., Chen, M., Zhu, Q., Zhou, L., Qin, W., Wang, T., 2017. Microcystin-LR promotes epithelial-mesenchymal transition in colorectal cancer cells through PI3-K/AKT and SMAD2. Toxicol. Lett. 265, 53–60. https://doi.org/10.1016/j.toxlet.2016.11.004.
Rhee, S.H., Bumseok, K., Lim, C.W., 2006. Morphologic changes in microcystin-LR treated hepatocytes in vitro. Journal of Toxicology and Public Health 22, 301–306.
Ribatti, D., Tamma, R., Annese, T., 2020. Epithelial-mesenchymal transition in cancer: a historical overview. Translational Oncology 13, 100773. https://doi.org/10.1016/j.tranon.2020.100773.
Roegner, A.F., Puschner, B., 2014. Aggregate culture: a more accurate predictor of microcystin toxicity for risk assessment. Toxicon 83, 1–14. https://doi.org/10.1016/j.toxicon.2014.02.017.
Rose, S., Cuvellier, M., Ezan, F., Carteret, J., Bruyère, A., Legagneux, V., Nesslany, F., Baffet, G., Langouët, S., 2022. DMSO-free highly differentiated HepaRG spheroids for chronic toxicity, liver functions and genotoxicity studies. Arch. Toxicol. 96, 243–258. https://doi.org/10.1007/s00204-021-03178-x.
Rose, S., Ezan, F., Cuvellier, M., Bruyère, A., Legagneux, V., Langouët, S., Baffet, G., 2021. Generation of proliferating human adult hepatocytes using optimized 3D culture conditions. Sci. Rep. 11, 515. https://doi.org/10.1038/s41598-020-80019-4.
Sedan, D., Giannuzzi, L., Rosso, L., Alberto Marra, C., Andrinolo, D., 2013. Biomarkers of prolonged exposure to microcystin-LR in mice. Toxicon 68, 9–17. https://doi.org/10.1016/j.toxicon.2013.03.002.
Serras, A.S., Rodrigues, J.S., Cipriano, M., Rodrigues, A.V., Oliveira, N.G., Miranda, J.P., 2021. A critical perspective on 3D liver models for drug metabolism and toxicology studies. Front. Cell Dev. Biol. 9, 626805 https://doi.org/10.3389/fcell.2021.626805.
Shi, L., Du, X., Liu, H., Chen, X., Ma, Y., Wang, R., Tian, Z., Zhang, S., Guo, H., Zhang, H., 2021. Update on the adverse effects of microcystins on the liver. Environ. Res. 195 https://doi.org/10.1016/j.envres.2021.110890.
Solter, P.F., Wollenberg, G.K., Huang, X., Chu, F.S., Runnegar, M.T., 1998. Prolonged sublethal exposure to the protein phosphatase inhibitor microcystin-LR results in multiple dose-dependent hepatotoxic effects. Toxicol. Sci. 44, 87–96. https://doi.org/10.1006/toxs.1998.2478.
Sun, B., Karin, M., 2013. Inflammation and liver tumorigenesis. Front. Med. 7, 242–254. https://doi.org/10.1007/s11684-013-0256-4.
Sun, F., Wang, J., Sun, Q., Li, F., Gao, H., Xu, L., Zhang, J., Sun, X., Tian, Y., Zhao, Q., Shen, H., Zhang, K., Liu, J., 2019. Interleukin-8 promotes integrin β3 upregulation and cell invasion through PI3K/Akt pathway in hepatocellular carcinoma. J. Exp. Clin. Cancer Res. 38, 449. https://doi.org/10.1186/s13046-019-1455-x.
Svirčev, Z., Lalić, D., Bojadžija Savić, G., Tokodi, N., Drobac Backović, D., Chen, L., Meriluoto, J., Codd, G.A., 2019. Global geographical and historical overview of cyanotoxin distribution and cyanobacterial poisonings. Arch. Toxicol. 93, 2429–2481. https://doi.org/10.1007/s00204-019-02524-4.
Takano, H., Takumi, S., Ikema, S., Mizoue, N., Hotta, Y., Shiozaki, K., Sugiyama, Y., Furukawa, T., Komatsu, M., 2014. Microcystin-LR induces anoikis resistance to the hepatocyte uptake transporter OATP1B3-expressing cell lines. Toxicology 326, 53–61. https://doi.org/10.1016/j.tox.2014.10.003.
Taniguchi, T., Zanetti-Yabur, A., Wang, P., Usyk, M., Burk, R.D., Wolkoff, A.W., 2020. Interindividual diversity in expression of organic anion uptake transporters in normal and cirrhotic human liver. Hepatology Communications 4, 739–752. https://doi.org/10.1002/hep4.1489.
Thakkar, N., Slizgi, J.R., Brouwer, K.L.R., 2017. Effect of liver disease on hepatic transporter expression and function. J. Pharmaceut. Sci. 106, 2282–2294. https://doi.org/10.1016/j.xphs.2017.04.053.
Trosko, J.E., 2021. On the potential origin and characteristics of cancer stem cells. Carcinogenesis 42, 905–912. https://doi.org/10.1093/carcin/bgab042.
Ufelmann, H., Kruger, T., Luckas, B., Schrenk, D., 2012. Human and rat hepatocyte toxicity and protein phosphatase 1 and 2A inhibitory activity of naturally occurring desmethyl-microcystins and nodularins. Toxicology 293, 59–67. https://doi.org/10.1016/j.tox.2011.12.011.
Ulvestad, M., Bjorquist, P., Molden, E., Asberg, A., Andersson, T.B., 2011. OATP1B1/1B3 activity in plated primary human hepatocytes over time in culture. Biochem. Pharmacol. 82, 1219–1226. https://doi.org/10.1016/j.bcp.2011.07.076.
Ulvestad, M., Darnell, M., Molden, E., Ellis, E., Asberg, A., Andersson, T.B., 2012. Evaluation of organic anion-transporting polypeptide 1B1 and CYP3A4 activities in primary human hepatocytes and HepaRG cells cultured in a dynamic three-dimensional bioreactor system. J. Pharmacol. Exp. Therapeut. 343, 145–156. https://doi.org/10.1124/jpet.112.195750.
Ulvestad, M., Nordell, P., Asplund, A., Rehnström, M., Jacobsson, S., Holmgren, G., Davidson, L., Brolén, G., Edsbagge, J., Björquist, P., Küppers-Munther, B., Andersson, T.B., 2013. Drug metabolizing enzyme and transporter protein profiles of hepatocytes derived from human embryonic and induced pluripotent stem cells. Biochem. Pharmacol. 86, 691–702. https://doi.org/10.1016/j.bcp.2013.06.029.
Vandesompele, J., Preter, K. De, Pattyn, F., Poper, B., Roy, N. Van, Paepe, A. De, Speleman, F., 2002. Accurate normalization of real-time quantitative RT-PCR data by geometric averaging of multiple internal control genes. Genome Biol. 3, 00341–003411.
Vidal, F., Sedan, D., D'Agostino, D., Lorena Cavalieri, M., Mullen, E., Parot Varela, M.M., Flores, C., Caixach, J., Andrinolo, D., 2017. Recreational exposure during algal

bloom in Carrasco Beach, Uruguay: a liver failure case report. Toxins. https://doi.org/10.3390/toxins9090267.

Walesky, C., Apte, U., 2015. Role of hepatocyte nuclear factor 4α (HNF4α) in cell proliferation and cancer. Gene Expr. 16, 101–108. https://doi.org/10.3727/105221615X14181438356292.

Wang, X., Zhu, Y., Lu, W., Guo, X., Chen, L., Zhang, N., Chen, S., Ge, C., Xu, S., 2023. Microcystin-LR-induced nuclear translocation of cGAS promotes mutagenesis in human hepatocytes by impeding homologous recombination repair. Toxicol. Lett. 373, 94–104. https://doi.org/10.1016/j.toxlet.2022.11.015.

Wang, Z., Li, B., Jiang, H., Ma, Y., Bao, Y., Zhu, X., Xia, H., Jin, Y., 2021. IL-8 exacerbates alcohol-induced fatty liver disease via the Akt/HIF-1α pathway in human IL-8-expressing mice. Cytokine 138, 155402. https://doi.org/10.1016/j.cyto.2020.155402.

WHO, 2020. Cyanobacterial Toxins: Microcystins (No. WHO/HEP/ECH/WSH/2020.6). World Health Organization, Geneva.

Willebrords, J., Crespo Yanguas, S., Maes, M., Decrock, E., Wang, N., Leybaert, L., da Silva, T.C., Veloso Alves Pereira, I., Jaeschke, H., Cogliati, B., Vinken, M., 2016. Structure, regulation and function of gap junctions in liver. Cell Commun. Adhes. 1–9. https://doi.org/10.3109/15419061.2016.1151875.

Woolbright, B.L., Williams, C.D., Ni, H., Kumer, S.C., Schmitt, T., Kane, B., Jaeschke, H., 2017. Microcystin-LR induced liver injury in mice and in primary human hepatocytes is caused by oncotic necrosis. Toxicon 125, 99–109. https://doi.org/10.1016/j.toxicon.2016.11.254.

Wu, Y.-L., He, Y., Shi, J.-J., Zheng, T.-X., Lin, X.-J., Lin, X., 2019. Microcystin-LR promotes necroptosis in primary mouse hepatocytes by overproducing reactive oxygen species. Toxicol. Appl. Pharmacol. 377, 114626 https://doi.org/10.1016/j.taap.2019.114626.

Yang, S., Chen, Z., Cheng, Y., Liu, T., Yin, Lihong, Pu, Y., Liang, G., 2021. Environmental toxicology wars: organ-on-a-chip for assessing the toxicity of environmental pollutants. Environ. Pollut. 268, 115861 https://doi.org/10.1016/j.envpol.2020.115861.

Zhang, B., Liu, Y., Li, X., 2015. Alteration in the expression of cytochrome P450s (CYP1A1, CYP2E1, and CYP3A11) in the liver of mouse induced by microcystin-LR. Toxins 7, 1102–1115. https://doi.org/10.3390/toxins7041102.

Zhao, Y., Xue, Q., Su, X., Xie, L., Yan, Y., Wang, L., Steinman, A.D., 2016. First identification of the toxicity of microcystins on pancreatic islet function in humans and the involved potential biomarkers. Environ. Sci. Technol. 50, 3137–3144. https://doi.org/10.1021/acs.est.5b03369.

Zheng, C., Zeng, H., Lin, H., Wang, J., Feng, X., Qiu, Z., Chen, J.-A., Luo, J., Luo, Y., Huang, Y., Wang, L., Liu, W., Tan, Y., Xu, A., Yao, Y., Shu, W., 2017. Serum microcystin levels positively linked with risk of hepatocellular carcinoma: a case-control study in southwest China. Hepatology 66, 1519–1528. https://doi.org/10.1002/hep.29310.